Title
A new technique for luminosity measurement using 3D pixel modules in the ATLAS IBL detector

Authors
Liu, Peilian
Collaboration, on behalf of the ATLAS

Publication Date
2019-04-01

DOI
10.1016/j.nima.2018.09.027

Peer reviewed

A new technique for luminosity measurement using 3D pixel modules in the ATLAS IBL detector

Peilian Liu[1], on behalf of the ATLAS Collaboration

Physics Division, Lawrence Berkeley National Laboratory, Berkeley, CA 94720, USA

Abstract

The Insertable B-Layer (IBL) is the innermost layer of the ATLAS tracking system. It consists of planar pixel modules in the central region and 3D pixel modules at the two extremities. We use the longitudinal cluster-size distributions in 3D modules of the IBL to determine the number of pixel clusters per bunch crossing produced by primary charged particles in randomly triggered collision events, and to suppress the associated backgrounds. This Pixel-Cluster-Counting algorithm can provide both bunch-integrated and bunch-by-bunch relative-luminosity measurements, and thereby contribute independent constraints to the understanding and the evaluation of the systematic uncertainties that dominate the luminosity determination at the ATLAS experiment.

Keywords: Luminosity, 3D Pixel Module, Pixel Cluster

1. Introduction

An accurate measurement of the delivered luminosity is a key component of the ATLAS [1] physics programme. For cross section measurements, the uncertainty in the delivered luminosity is often one of the major systematic uncertainties. Searches for, and eventual discoveries of, physical phenomena beyond the Standard Model also rely on accurate information about the delivered luminosity to evaluate background levels and determine sensitivity to the signatures of new phenomena.

In LHC Run 2, the primary ATLAS luminometer is LUCID [2], a photomultiplier-based Cherenkov detector specifically designed to measure the bunch-by-bunch luminosity in every bunch crossing. It is complemented by bunch-by-bunch luminosity-sampling algorithms such as track counting,

[1]Corresponding author, email: peilianliu@lbl.gov

as well as by several bunch-integrating algorithms that do not provide information on individual colliding-bunch pairs. The measurements of these luminometers are compared to assess and control the systematic uncertainties of the luminosity measurements at ATLAS. The level of consistency across the various methods, over the full range of luminosities and beam conditions, and across many months of LHC operation, provides a direct test of the accuracy and the stability of the results. New algorithms such as Pixel-Cluster-Counting (PCC) can provide additional, independent constraints on the understanding of some of the instrumental biases (such as long-term drifts, or the pileup dependence of luminosity measurements) and to the evaluation of the associated systematic uncertainties. This algorithm has been significantly improved since the first presentation in Ref. [3].

2. Principle of the luminosity measurement in ATLAS

The bunch luminosity $\mathcal{L}_{\mathrm{b}}$ produced by a single pair of colliding bunches can be expressed as

$$\mathcal{L}_{\mathrm{b}} = \frac{\mu f_{\mathrm{r}}}{\sigma_{\mathrm{inel}}} \tag{1}$$

where the pileup parameter μ is the average number of inelastic interactions per bunch-crossing, f_{r} is the bunch revolution frequency (11245.5 Hz at LHC), and σ_{inel} is the pp inelastic cross section.

ATLAS monitors the delivered luminosity by measuring μ_{vis}, the visible interaction rate per bunch crossing (BC). The bunch luminosity can then be written as

$$\mathcal{L}_{\mathrm{b}} = \frac{\mu_{\mathrm{vis}} f_{\mathrm{r}}}{\sigma_{\mathrm{vis}}} \tag{2}$$

where $\mu_{\mathrm{vis}} = \varepsilon\mu$, ε is the efficiency of the detector and algorithm under consideration, and the visible cross section for that same detector and algorithm is defined by $\sigma_{\mathrm{vis}} = \varepsilon\sigma_{\mathrm{inel}}$. μ_{vis} is a directly measurable quantity. The visible cross section σ_{vis} is calibrated by the van der Meer (vdM) method [2] under specialized beam conditions.

3. Insertable B-Layer

The ATLAS pixel detector is the innermost detector component of the ATLAS tracking system. Currently, the pixel-detector layer closest to the

Table 1: η and ϕ indices of the 3D and planar modules from the negative-z side of IBL to the positive-z side. The IBL is constructed of 14 staves each of which consists of 20 modules.

Structure	3D	Planar	3D
η index	-10 $\rightarrow$ -7	-6 $\rightarrow$ 5	6 $\rightarrow$ 9
ϕ index	0 $\rightarrow$ 13		

beam pipe is the insertable b-layer (IBL) [4], which was installed in 2014 between the existing pixel detector and a new smaller radius beam-pipe at a radius of 3.3 cm, to maintain the performance of the pixel detector with increasing luminosity. The IBL is constructed of 14 staves laid around the beam pipe. Each IBL stave is instrumented along 64 cm and consists of 20 modules, with four 3D sensor modules at each end and 12 planar sensor modules in the central section. Planar sensors are conventional devices made with surface implants and uniform bulk, and 3D sensors use implants vertically through the bulk [5]. Table 1 lists the η and ϕ indices of the 3D and planar modules[1].

In each 3D module, one FE-I4B chip [6] is bump bonded to one 3D sensor. There are 26880 pixels arranged in 80 columns on 250 μm pitch by 336 rows on 50 μm pitch. The 3D sensor thickness is 230 μm.

4. Pixel-Cluster Counting Algorithm

The principle of the PCC-based luminosity measurement is that the number of clusters produced by primary particles (referred to as "primary clusters") is assumed to be proportional to the luminosity. The absolute PCC luminosity scale is fixed by cross-calibrating it to LUCID in a reference run.

Only primary clusters in the 3D modules of the IBL, that are produced by primary particles from *pp* collisions, are counted. The number of background

[1]ATLAS uses a right-handed coordinate system with its origin at the nominal interaction point in the centre of the detector, and the z-axis along the beam line. The x-axis points from the interaction point to the centre of the LHC ring, and the y-axis points upwards. Cylindrical coordinates (r, ϕ) are used in the transverse plane, ϕ being the azimuthal angle around the beam line. The pseudorapidity is defined in terms of the polar angle θ as $\eta = -\ln\tan(\frac{\theta}{2})$.

clusters depends not only on the luminosity, but also on beam conditions and on material effects. The 3D modules are located at high $|\eta|$. Particles from the interaction point (IP) traverse 3D modules at shallow incidence, producing long clusters, which is key to signal-background separation. Figure 1 compares the experimental longitudinal cluster size distributions for the four 3D modules at positive-z (η indexed 6 through 9). The primary clusters contribute to the Gaussian component while the background clusters are shorter.

The module farthest from the interaction point (η indexed 9) sees the longest primary clusters. Data-volume constraints prevent saving all the pixel clusters in the entire IBL detector with reconstructed data. 3D modules were selected for saving all pixel clusters (as required for PCC) because they have the best signal-to-background ratio, due to their high $|\eta|$ location. Additionally, the 3D modules extend beyond the $|\eta| < 2.5$ acceptance of the rest of the ATLAS tracker, which makes PCC independent of the track-based luminosity measurement. There is an average of ~ 0.02 clusters produced in one 3D module by one event, so the probability of two particles producing overlapping clusters is low.

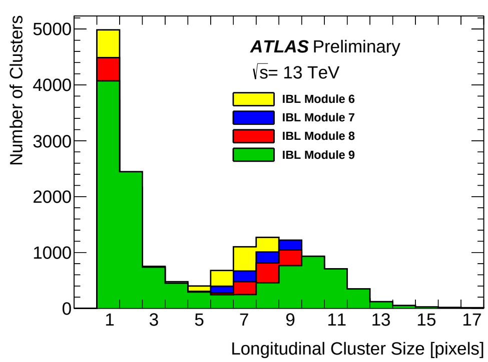

Figure 1: Comparison of longitudinal cluster size distributions for the four most forward 3D modules on the positive-z side of IBL.

4.1. Gaussian distribution of the longitudinal cluster size for the primary clusters

The longitudinal size of primary clusters is sensitive to the particle incidence angle, and could be calculated by

$$\text{Longitudinal size} = \frac{\text{sensor thickness}}{\text{pixel pitch}} \cdot \frac{z_{\text{IP}} - z_{\text{3D}}}{r_{\text{IBL}}} \tag{3}$$

Here z_{3D} is the z position of the 3D module, z_{IP} is where the interaction occurs in the z direction, and r_{IBL} is the radius of the IBL. Since the z_{IP} distribution is approximately Gaussian, the longitudinal cluster size distribution of individual 3D modules is also expected to exhibit an approximately Gaussian shape.

The primary clusters produced on the module edge are shorter than expected due to missing pixels. Similarly, clusters can be interrupted (broken) by dead or inefficient pixels. Figure 2 illustrates the longitudinal size distributions of broken and on-edge primary clusters as well as of complete primary clusters. The shapes were obtained from simulated single-interaction minimum-bias events. In collision data, on-edge clusters are avoided by requiring cluster centers to be a minimum distance away from an edge. This defines a fiducial area for each module. Broken clusters with a gap of a single pixel constitute about 5.6% of all primary clusters, and they are removed from the analysis.

4.2. Background clusters

In the products of *pp* collisions, aside from the primary particles produced in the primary collisions, there are secondary particles from the interaction of the primary particles and photons with the detector material, as well as beam backgrounds. These lead to background clusters. There are also 1-hit background clusters from noisy pixels. In addition, when charged particles travel through the detector, they can activate the detector material. This radioactivity causes small hits to be seen in the detector. It decays away after a brief period of time. This “afterglow” effect is studied in special runs in which several empty BCs are collected after the paired BC. The afterglow effects contribute short clusters. In clusters longer than two pixels, the background clusters from afterglow effects and noisy pixels are expected to be negligible and treated as a systematic uncertainty.

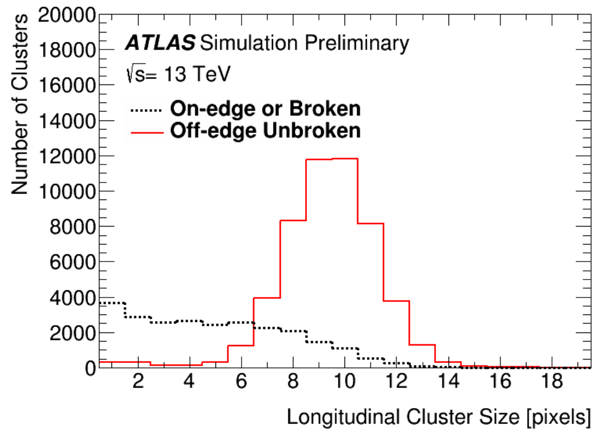

Figure 2: Longitudinal size distributions of primary clusters in the most forward IBL 3D module on the negative-z side, obtained from simulated single-interaction minimum-bias events. Only clusters originating from primary particles are used.

4.3. Extraction of the number of primary clusters in each 3D module

A two-component fit is performed to the longitudinal cluster size distribution, as illustrated in Figure 3. Clusters on the module edges and broken clusters have been removed. The fit components are a Gaussian to describe the signal clusters from primary particles and a template to describe the background clusters from secondary particles. The background template is derived from the minimum bias MC sample with one interaction per BC by selecting the pixel clusters originating from the secondary particles with the same selection as for the data. Clusters shorter than three pixels are excluded from the fit to minimize the systematic uncertainty from background sources that are not simulated, such as afterglow and noisy pixels.

4.4. Exclusion of modules suffering performance issues

A plain average of all modules at the same η can be biased when a module has a transient problem. In order to exclude such modules, we fit the azimuthal distribution of the number of primary clusters per module (integral of the Gaussian component of the fit described in Sec. 4.3) for the 14 modules at the same η (same index), to a cosine function excluding outliers:

$$\text{Number of clusters} = A \cdot \cos(\frac{2\pi}{14}(\text{ID}_\phi - B)) + C, \tag{4}$$

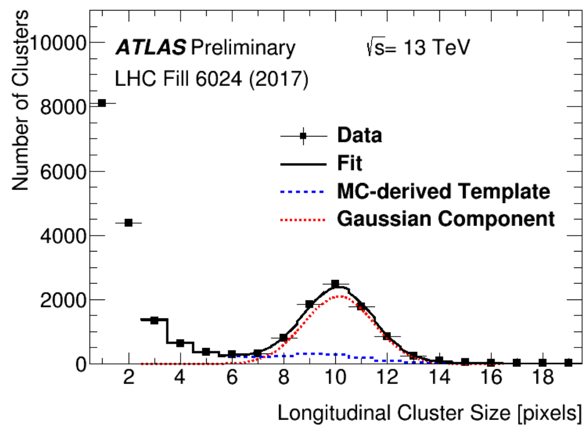

Figure 3: Two-component fit to the longitudinal cluster size distribution of clusters longer than two pixels in the most forward IBL 3D module on the negative-z side. The data correspond to about one minute of data-taking and are extracted from randomly triggered events.

A cosine fit is needed to account for the beams not being perfectly centered in the IBL. ID_ϕ is the ϕ index of each module in the same η ring, which ranges from 0 to 13. B is the ϕ index of the module closest to the IP in the transverse plane, and is fixed to the value calculated from the reconstructed transverse position of the luminous centroid. This fixes the phase of the cosine to its known value. In the example shown in Figure 4, the module at ϕ index 8 has been excluded as an outlier. The area under the fitted curve is then taken as the correct cluster count in one η ring and is used as a proxy to estimate the luminosity.

4.5. Geometric-acceptance correction

The geometric acceptance of each module varies depending on the source point of the primary particles considered. The distribution of primary interaction vertices (known from track reconstruction) can therefore be used to correct for the precise acceptance of each module in each luminosity block (approximately 1 minute of data) analyzed. The transverse distribution is tightly constrained by the $\sim 10\,\mu$m transverse beam size and the effect of the transverse beam position is accounted for in the sinusoidal fit described above. Therefore, we correct here for the distribution of the longitudinal position z_{IP} of individual collisions, as reflected in the mean longitudinal position and RMS spread of the luminous region.

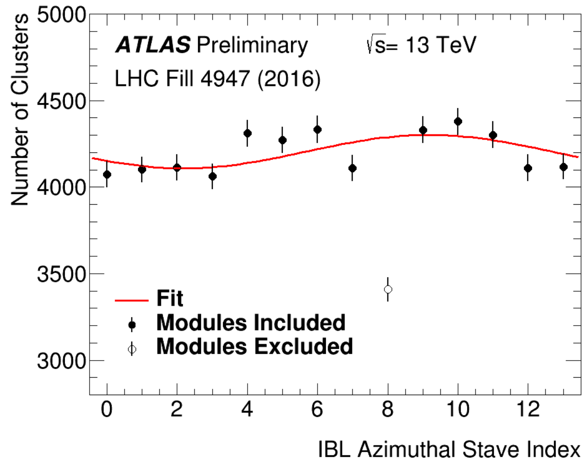

Figure 4: Azimuthal dependence of the number of primary clusters for the modules in the most forward IBL η ring on the negative-z side. The data correspond to about one minute of data-taking and are extracted from randomly triggered events.

In Figure 5, simulated single-interaction minimum-bias events are used to study how the number of clusters depends on z_{IP}. The positive and negative modules behave inversely along z_{IP} as expected. The distribution of all clusters in all 3D modules produced by one interaction (n) as a function of z_{IP} is fitted with:

$$n = n_0 \cdot (1 + p_2 \cdot (z_{\mathrm{IP}} - z_0)^2) \tag{5}$$

n_0 is the total number of primary clusters produced by one interaction happening at the IBL center z_0.

As already mentioned, the z_{IP} distribution of the multiple (μ) interactions in each BC is a Gaussian: $\mathrm{Gauss}(z_{\mathrm{IP}}; m_z, \sigma_z)$, where m_z is the longitudinal position of the luminous centroid and σ_z is the luminous length. The total number of clusters in all 3D modules produced by all interactions in the luminous region is obtained by integrating Equation (5) along $\mathrm{Gauss}(z_{\mathrm{IP}}; m_z, \sigma_z)$:

$$\begin{aligned} N &= \int n_0 \cdot (1 + p_2 \cdot (z_{\mathrm{IP}} - z_0)^2) \cdot \mu \cdot \mathrm{Gauss}(z_{\mathrm{IP}}; m_z, \sigma_z) dz_{\mathrm{IP}} \qquad (6) \\ &= n_0 \cdot \mu \cdot (1 + p_2 \cdot ((m_z - z_0)^2 + \sigma_z^2)) \qquad (7) \\ &= N_0 \cdot (1 + p_2 \cdot ((m_z - z_0)^2 + \sigma_z^2)) \qquad (8) \end{aligned}$$

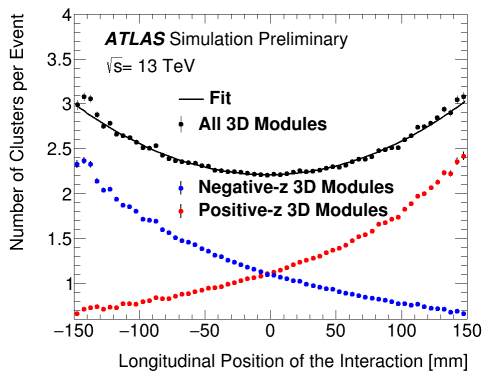

(a)

Figure 5: Number of clusters in the 3D modules on the positive-z (red) and the negative-z (blue) side of the IBL as a function of the longitudinal position of the interaction, obtained from simulated single-interaction minimum-bias events. The distribution of all clusters is fitted with a second-order polynomial.

$N_0 = n_0 \cdot \mu$ would be the number of observed clusters if all the interactions happened exactly at z_0. A longer or longitudinally off-center luminous region produces more clusters. BCs with identical luminosity produce different number of clusters, N, if they have luminous regions of different shapes or positions. Therefore, we always correct N to the ideal N_0 using the known shape of the luminous region:

$$N_0 = \frac{N}{1 + p_2 \cdot ((m_z - z_0)^2 + \sigma_z^2)} \tag{9}$$

The effect of this correction is shown in Figure 6.

5. Validation of the PCC method

The principle of the PCC algorithm is that the number of primary clusters is assumed to be proportional to the luminosity. To validate this assumption, the corrected number of pixel clusters in all 3D modules (N_0) is compared with the luminosity measured by LUCID ($\mathcal{L}_{\mathrm{LUCID}}$). The history of the $N_0/\mathcal{L}_{\mathrm{LUCID}}$ ratio over LHC fill 6024 is presented in Figure 7. The value of N_0, integrated over the duration of the fill, is normalized to the LUCID-based integrated luminosity over the same period, to derive the PCC-based luminosity ($\mathcal{L}_{\mathrm{PCC}}$) in one-minute bins. $\mathcal{L}_{\mathrm{PCC}}/\mathcal{L}_{\mathrm{LUCID}}$ is constant over LHC fill 6024. In this fill,the bunch-averaged pileup parameter $< \mu >$ ranges from $\sim$40 to $\sim$16. Therefore, $\mathcal{L}_{\mathrm{PCC}}/\mathcal{L}_{\mathrm{LUCID}}$ is independent of $< \mu >$.

6. Summary

A relative-luminosity monitoring technique based on pixel-cluster counting in the forward modules of the ATLAS IBL has been developed. The signal clusters (produced by the primary particles) are separated from backgrounds (mainly produced by secondary particles) by fitting the longitudinal cluster size distribution in the IBL 3D modules. Occasional readout failures of individual 3D modules are mitigated on the basis of the internal consistency of the azimuthal distribution of the number of clusters for the 14 modules at the same η. Geometric-acceptance effects associated with the imperfect centering and finite longitudinal extent of the luminous region are corrected using simulated collisions. The method has been validated on 2016 and 2017 ATLAS data at $\sqrt{s} = 13\,\mathrm{TeV}$, and its implementation in the overall luminosity analysis is well advanced. The PCC algorithm will contribute to the constraint of the systematic uncertainty of luminosity measurements.

7. Acknowledgements

This work was supported by the U.S. Department of Energy, Office of Science under contract DE-AC02-05CH11231.

8. References

[1] ATLAS Collaboration, The ATLAS Experiment at the CERN Large Hadron Collider, JINST 3 (2008) S08003.

[2] ATLAS Collaboration, Luminosity determination in pp collisions at $\sqrt{s} = 8\,\mathrm{TeV}$ using the ATLAS detector at the LHC, Eur. Phys. J. C 76 (2016) 653.

[3] ATLAS collaboration, Pixel-Cluster Counting Luminosity Measurements In ATLAS, PoS ICHEP2016 (2017) 1064.

[4] ATLAS Collaboration, ATLAS Insertable B-Layer Technical Design Report, ATLAS-TDR-19, CERN/LHCC 2010-013, 2010.

[5] P. Grenier, Silicon sensor technologies for the ATLAS IBL upgrade, TIPP2011 Conference Proceeding in press in Physics Procedia (2011).

[6] M. Garcia-Sciveres et al., The FE-I4 pixel readout integrated circuit, Nuclear Instruments and Methods in Physics Research A 636 (2011) S155-S159.

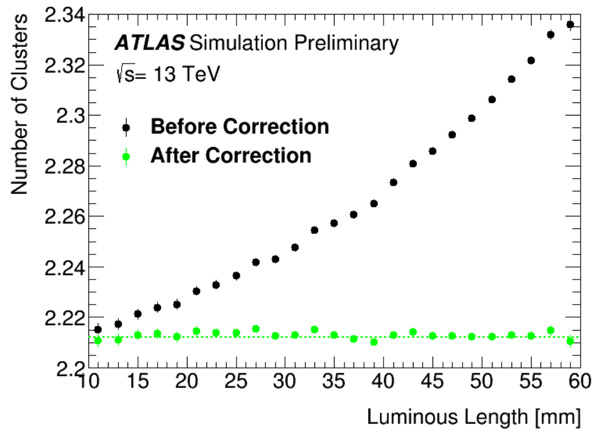

(a)

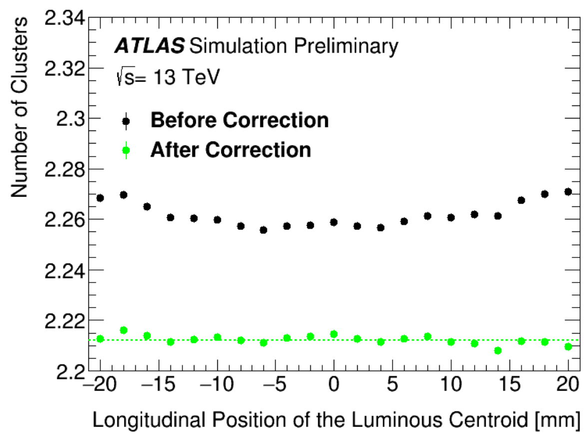

(b)

Figure 6: (a) Luminous-length dependence of the total number of primary clusters per inelastic collision, in the 3D modules of the IBL. The black points show the number of clusters obtained in the simulated minimum-bias samples, N, for different values of the luminous length (σ_z) but the same longitudinal position of the luminous centroid ($m_z =$ -2 mm). The green points show the corrected number of clusters, N_0. (b) Dependence on the longitudinal position of the luminous centroid, of the total number of primary clusters per inelastic collision in the 3D modules of the IBL. The black points show the number of clusters, N, obtained in the simulated minimum-bias samples for different longitudinal positions (m_z) of the luminous centroid, but with the same luminous length ($\sigma_z = 35$ mm). The green points show the corrected number of clusters, N_0. The dashed lines show the expected number of clusters, N_0, if all the interactions happened exactly at z_0.

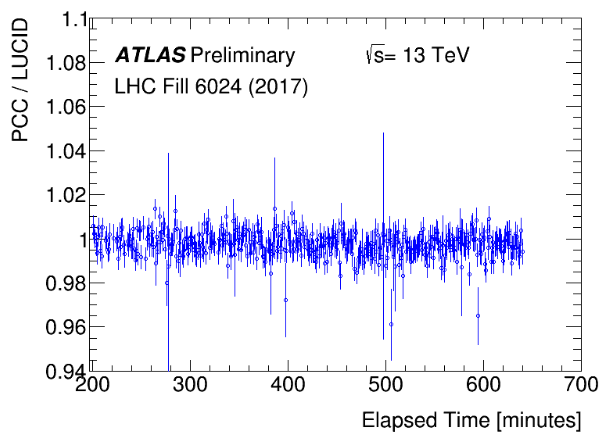

Figure 7: Stability of the PCC/LUCID luminosity ratio over the course of LHC fill 6024. The errors represent only the statistical error, which is dominated by PCC. The LUCID statistical uncertainty is negligible.